

# Supplementary Material

## 1 SUPPLEMENTARY PSEUDOCODE

**Result:** Estimated winter-balance field  $\hat{b}_w(x, y)$ ,  $\hat{B}_w$  and RMSE evaluated against real data for each glacier, survey design, number of sampling locations  $N$  and quasi-regular/irregular sample spacing

```

for  $i \rightarrow 1$  to 3 glaciers ( $G4, G2, G13$ ) do
  for  $j \rightarrow 1$  to 6 survey designs ( $CL, CT, CR, HG, HC, RN$ ) do
    for  $N \rightarrow 6$  to  $N_{\max}$  samples do
      if irregular sample spacing then
        for  $k \rightarrow 1$  to 200 sampling configurations do
          for  $l \rightarrow 1$  to  $l_{\max}$  trials do
            Select  $N$  random sampling locations;
            Compute distances between sampling locations;
            Store maximum value;
          end
          Identify maximin* design (one of  $l_{\max}$  configurations of  $N$  sampling locations);
          Determine regression parameters  $\beta_0, \beta_i, \epsilon$  (Equation 1);
          Estimate winter balance field  $\hat{b}_w(x, y)$  and  $\hat{B}_w$ ;
          Compute RMSE (Equation 2) using all measurement locations;
        end
      else
        Identify maximin* design for  $N$  sampling locations;
        Determine regression parameters  $\beta_0, \beta_i, \epsilon$  (Equation 1);
        Estimate winter balance  $\hat{b}_w(x, y)$  and  $\hat{B}_w$ ;
        Compute RMSE (Equation 2) using all measurement locations;
      end
    end
  end
end

```

**Algorithm 1:** Algorithm used for real data.  $l_{\max}$  ranges from 100 to 1000.  $N_{\max}$  is the number of measured gridcells and depends on the survey design. \*The “maximin” design maximizes the minimum distance between samples (Johnson et al., 1990).

**Result:** Estimated winter-balance field  $\hat{b}_w(x, y)$ ,  $\hat{B}_w$  and RMSE evaluated against 200 synthetic datasets based on McGrath et al. (2015) or Pulwicky et al. (2018) for each glacier, survey design, number of sampling locations  $N$  and quasi-regular/irregular sample spacing

```

for  $i \rightarrow 1$  to 3 glaciers ( $G4, G2, G13$ ) do
  for  $d \rightarrow 1$  to 200 synthetic winter-balance fields do
    Sample  $\beta_i$  (McGrath et al., 2015), (Pulwicky et al., 2018) and  $\beta_0$  (Pulwicky et al., 2018)
    distributions;
    Generate synthetic winter-balance field with linear regression (Equation 1 with  $\epsilon = 0$ );
    for  $j \rightarrow 1$  to 6 survey designs ( $CL, CT, CR, HG, HC, RN$ ) do
      for  $N \rightarrow 6$  to  $N_{\max}$  samples do
        if irregular sample spacing then
          for  $k \rightarrow 1$  to 200 sampling configurations do
            for  $l \rightarrow 1$  to  $l_{\max}$  trials do
              Select  $N$  random sampling locations;
              Compute distances between sampling locations;
              Store maximum value;
            end
            Identify maximin* design (one of  $l_{\max}$  configurations of  $N$  sampling locations);
            Determine new regression parameters  $\beta_0, \beta_i, \epsilon$  (Equation 1);
            Estimate winter balance field  $\hat{b}_w(x, y)$  and  $\hat{B}_w$ ;
            Compute RMSE (Equation 2) using all gridcells in ablation area;
          end
        else
          Identify maximin* design for  $N$  sampling locations;
          Determine regression parameters  $\beta_0, \beta_i, \epsilon$  (Equation 1);
          Estimate winter balance field  $\hat{b}_w(x, y)$  and  $\hat{B}_w$ ;
          Compute RMSE (Equation 2) using all gridcells in ablation area;
        end
      end
    end
  end
end

```

**Algorithm 2:** Algorithm used for synthetic data.  $l_{\max}$  ranges from 100 to 1000.  $N_{\max}$  is the number of measured gridcells and depends on the survey design. \*The “maximin” design maximizes the minimum distance between samples (Johnson et al., 1990).

## 2 SUPPLEMENTARY FIGURES: METHODS

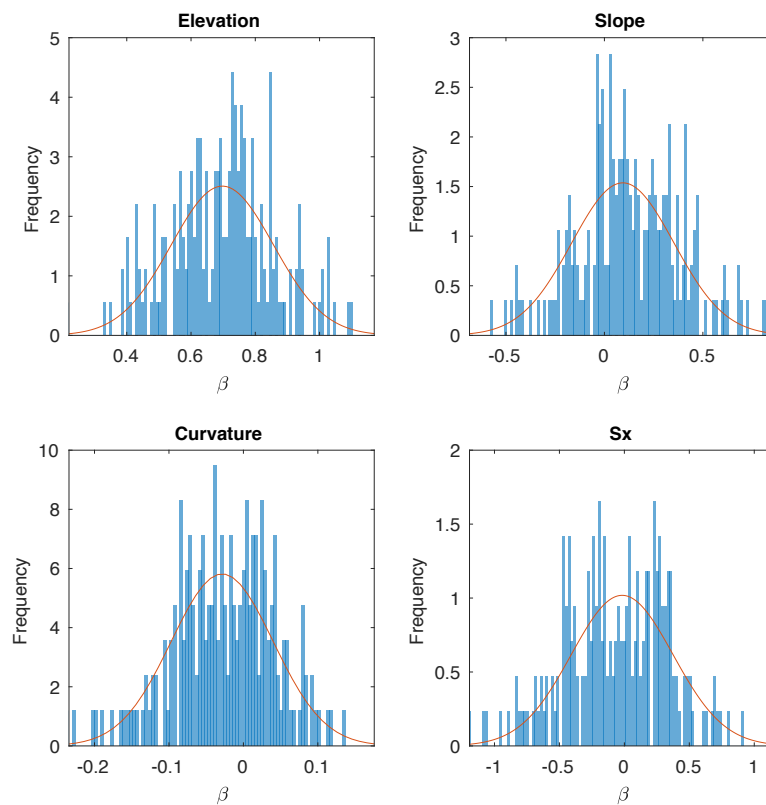


**Figure S1.** Normal distributions of  $\beta_i$  (curves) based on McGrath et al. (2015), randomly sampled (blue histograms) to generate synthetic winter-balance fields. Each coefficient  $\beta_i$  multiplies a topographic parameter (elevation, slope, curvature,  $S_x$ , as labelled) in the linear regression (Equation 1 in main text). Values of  $\beta_i$  are scaled such that magnitudes can be compared across topographic parameters. Random error ( $\epsilon$  in Equation 1) is added by sampling a normal distribution of zero mean and standard deviation equal to that determined for the subgrid variability of winter balance for each glacier by Pulwinski et al. (2018).

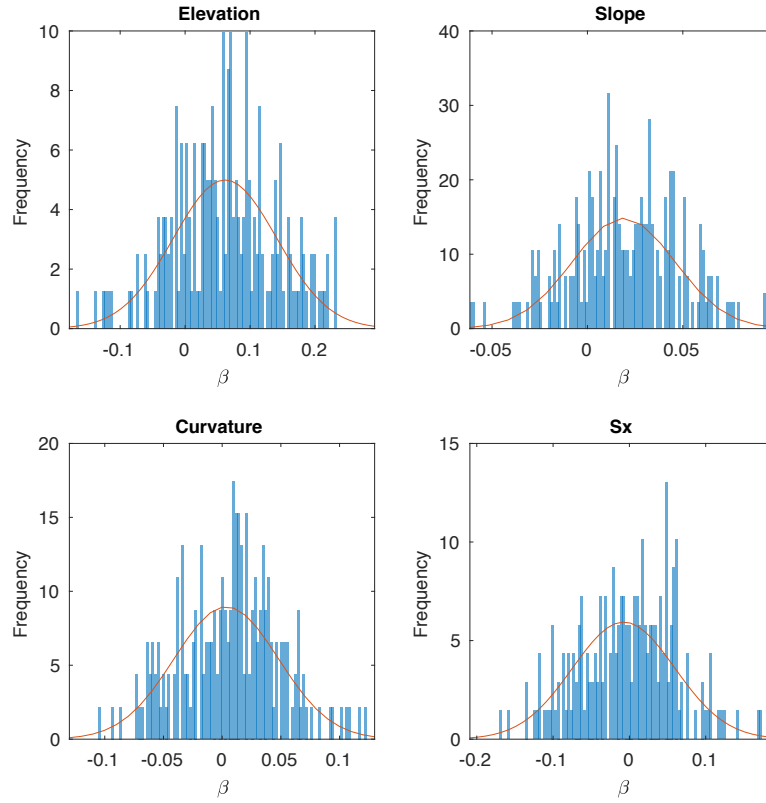


**Figure S2.** Normal distributions of  $\beta_i$  (curves) based on Pulwinski et al. (2018), randomly sampled (blue histograms) to generate synthetic winter-balance fields. Each coefficient  $\beta_i$  multiplies a topographic parameter (elevation, slope, curvature,  $S_x$ , as labelled) in the linear regression (Equation 1 in main text). Values of  $\beta_i$  are scaled such that magnitudes can be compared across topographic parameters. Random error ( $\epsilon$  in Equation 1) is added by sampling a normal distribution of zero mean and standard deviation equal to that determined for the subgrid variability of winter balance for each glacier by Pulwinski et al. (2018).



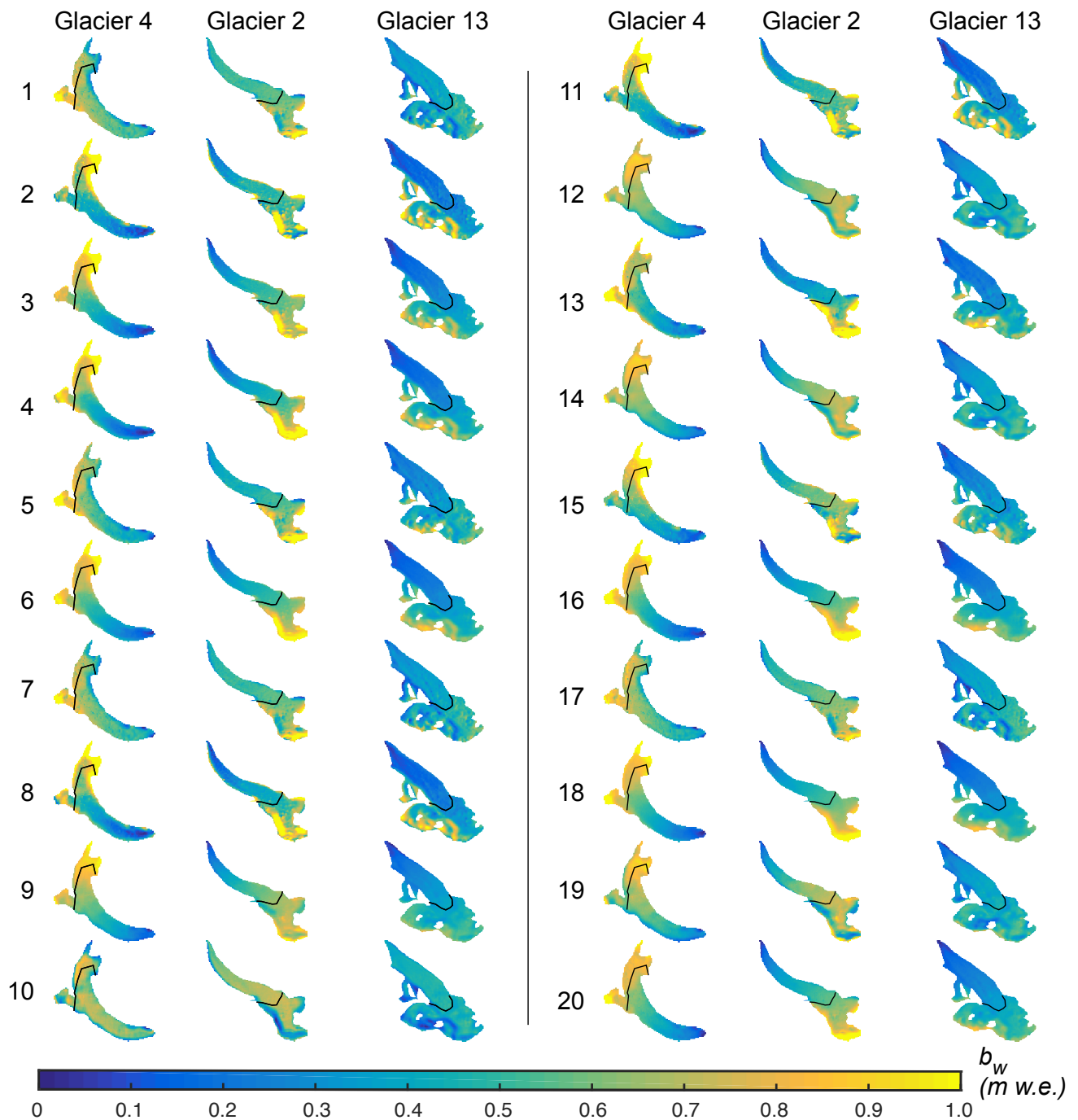


**Figure S3.** Ten percent of the synthetic winter-balance fields based on McGrath et al. (2015). The same values of coefficients  $\beta_i$  were applied to each glacier in each of the 200 fields generated (20 shown here). Random error  $\epsilon$  is glacier-specific. Approximate ELAs shown as black lines. Glaciers not plotted to scale.

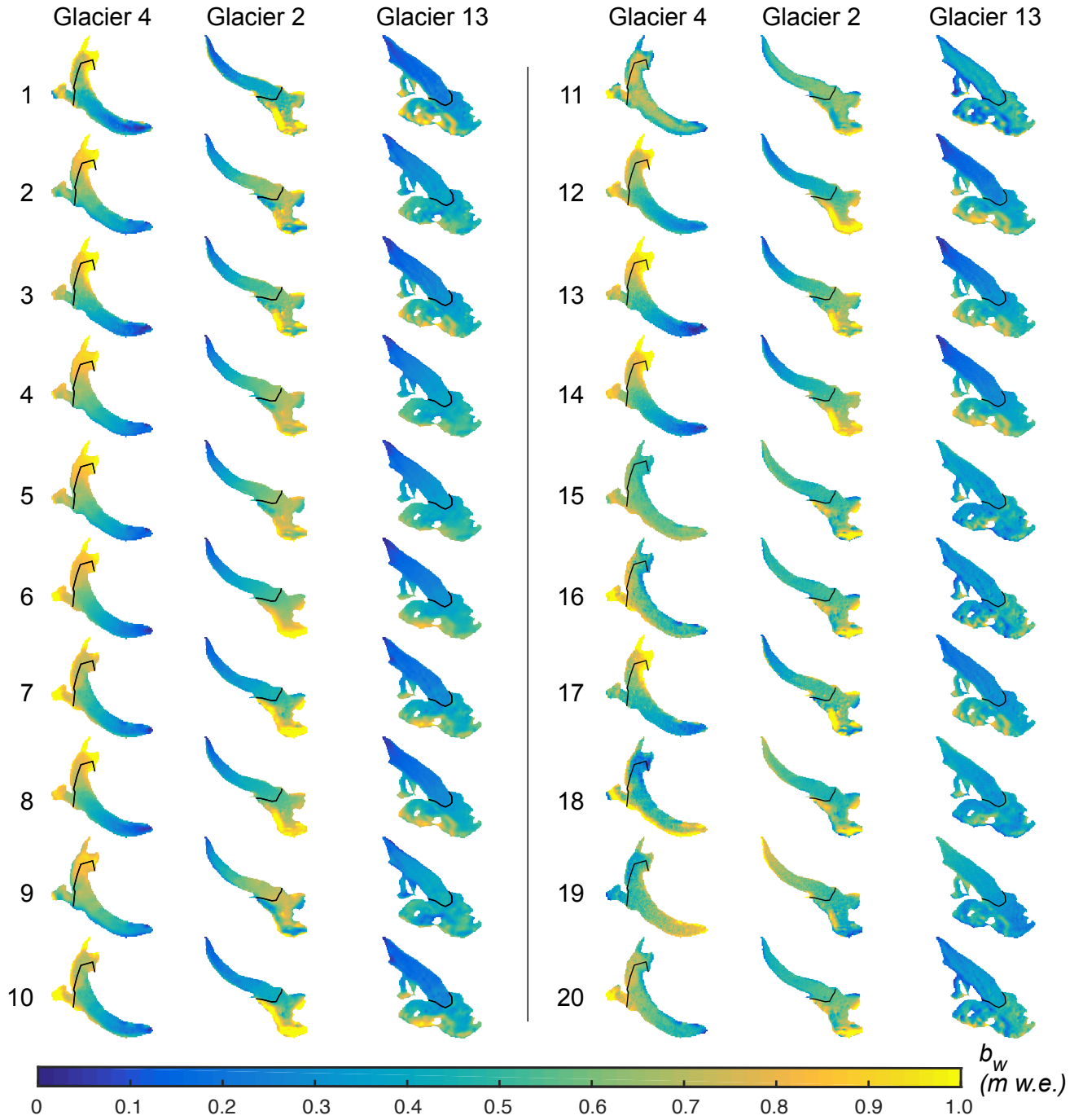


**Figure S4.** Ten percent of the synthetic winter-balance fields based on Pulwinski et al. (2018). The same values of coefficients  $\beta_i$  were applied to each glacier in each of the 200 fields generated (20 shown here). Random error  $\epsilon$  is glacier-specific. Approximate ELAs shown as black lines. Glaciers not plotted to scale.

### 3 SUPPLEMENTARY FIGURES: RESULTS

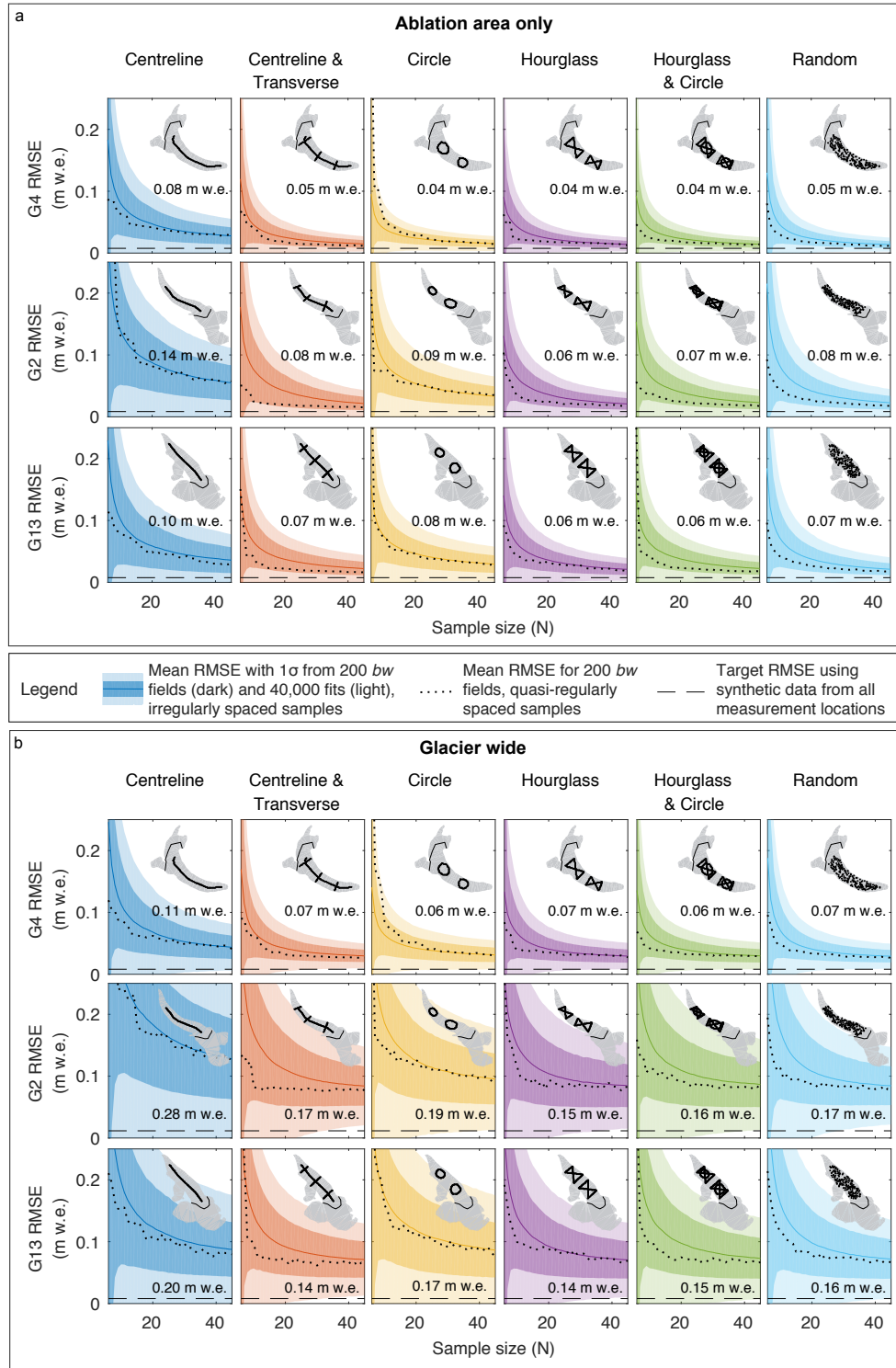


**Figure S5.** RMSEs for synthetic data (based on Pulwinski et al. (2018)) computed on a gridcell-by-gridcell basis across the ablation area (a) and glacier wide (b) between known (synthetic) winter balance and that estimated using subsets of the synthetic data in a linear topographic regression (Equation 1), for various survey designs (columns) and sample sizes  $N$  (x-axes) for Glacier 4 (top rows), Glacier 2 (middle rows) and Glacier 13 (bottom rows). Insets show example sampling configurations. Bold coloured lines are mean values of RMSE from 200 estimates of each of the 200 synthetic winter-balance fields using different configurations of irregularly spaced synthetic samples (40,000 model fits); values are given for  $N = 10$ . Light shading indicates the standard deviation arising from the 40,000 fits. Dotted lines are mean values of RMSE from estimates of each of the 200 synthetic winter-balance fields using quasi-regularly spaced synthetic samples. Dark shading indicates the standard deviation arising from the 200 different winter-balance fields. Horizontal dashed lines are the target RMSEs when synthetic data from all measurement locations are used to estimate winter balance. The proximity of the RMSE to the dashed line is a measure of precision, while its proximity to zero is a measure of accuracy.

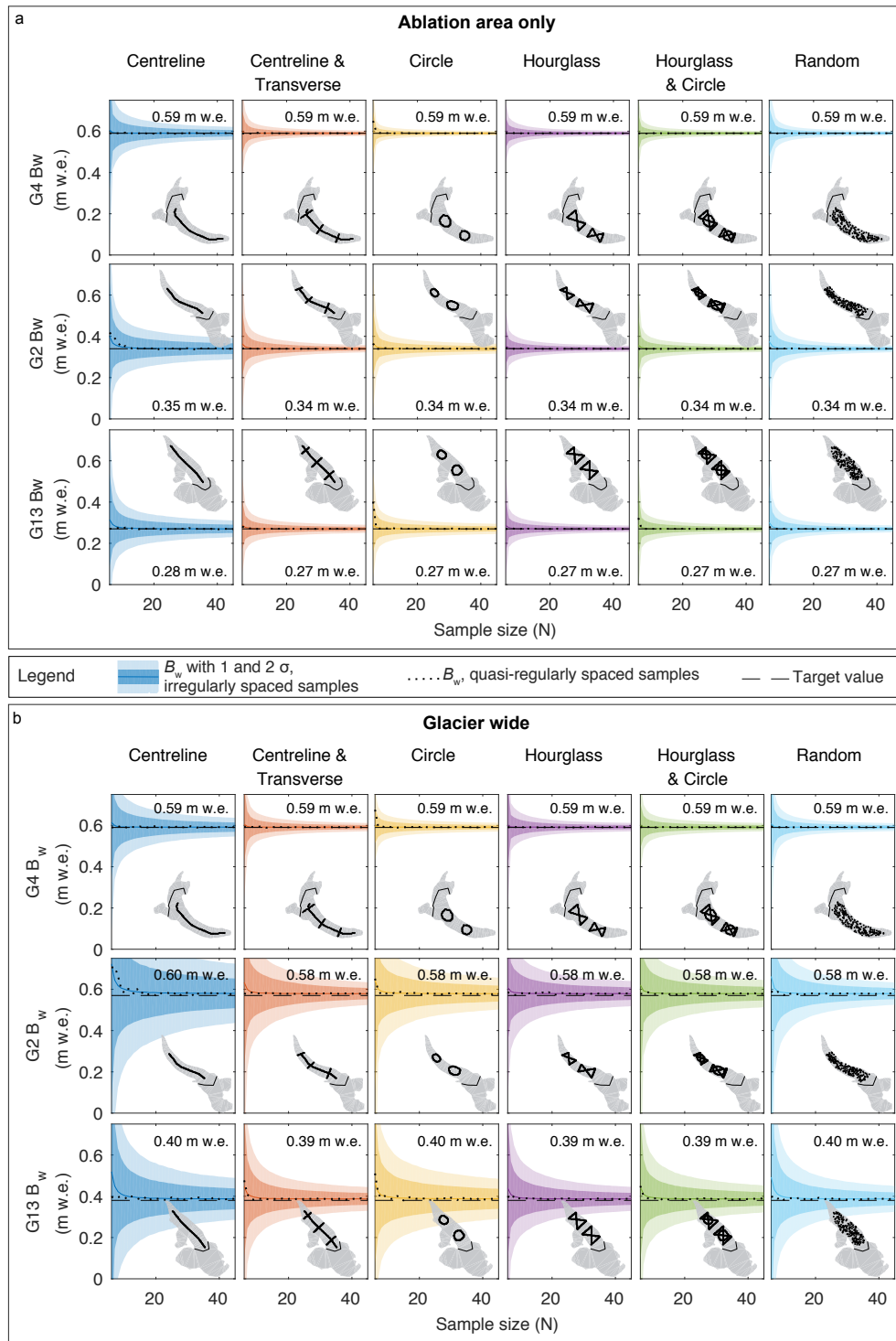


**Figure S6.** Ablation-area-wide (a) and glacier-wide (b) winter balance  $B_w$  estimated using synthetic data (based on Pulwinski et al. (2018)) in a linear topographic regression, for various survey designs (columns) and sample sizes  $N$  (x-axes) for Glacier 4 (top rows), Glacier 2 (middle rows) and Glacier 13 (bottom rows). Insets show example sampling configurations. Bold coloured lines are mean values of 200 estimates of  $B_w$  from each of the 200 synthetic winter-balance fields using different configurations of irregularly spaced synthetic samples (40,000 model fits); values are given for  $N = 10$ . Light shading indicates the standard deviation arising from the 40,000 fits. Dark shading indicates the standard deviation arising from the 200 different winter-balance fields. Horizontal dashed lines are the target values of  $B_w$ . Dotted lines are mean values of  $B_w$  from estimates of each of the 200 synthetic winter-balance fields using quasi-regularly spaced synthetic samples.

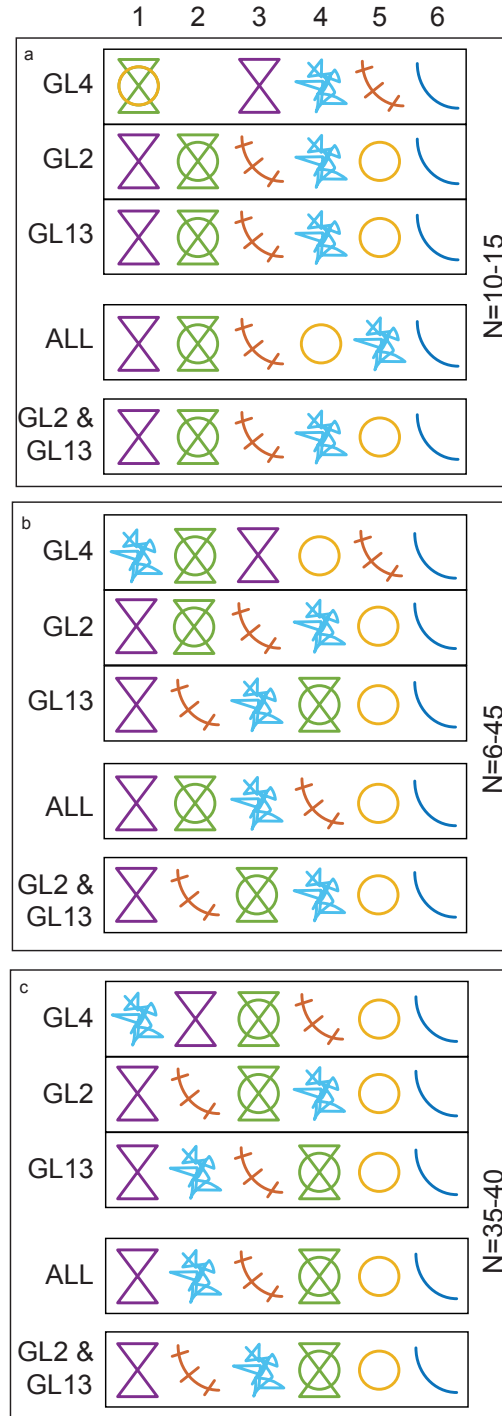


**Figure S7.** Ranking of survey designs from 1 to 6 (best to worst, left to right) using synthetic data (based on Pulwinski et al. (2018)) for (a) low  $N$  (10–15 sampling locations, upper block), (b) wide range of  $N$  (6–45 sampling locations, middle block) and (c) high  $N$  (35–40 sampling locations, lower block). Rankings are based on RMSE for  $b_w$  across the ablation area, for a given survey design averaged over the specified range of  $N$ . Results are shown for Glaciers 4, 2, 13 individually (G4, G2, G13), together (ALL) and for Glaciers 2 and 13 combined (G2 & G13). From left to right in second row, symbols represent HG, HC, CT, RN, CR, CL.

---

## REFERENCES

- Johnson, M., Moore, L., and Ylvisaker, D. (1990). Minimax and maximin distance designs. *Journal of Statistical Planning and Inference* 26, 131–148
- McGrath, D., Sass, L., O’Neel, S., Arendt, A., Wolken, G., Gusmeroli, A., et al. (2015). End-of-winter snow depth variability on glaciers in Alaska. *Journal of Geophysical Research: Earth Surface* 120, 1530–1550. doi:10.1002/2015JF003539
- Pulwinski, A., Flowers, G. E., Radić, V., and Bingham, D. (2018). Estimating winter balance and its uncertainty from direct measurements of snow depth and density on alpine glaciers. *Journal of Glaciology* 64, 781–795